

Irradiated ocean planets bridge super-Earth and sub-Neptune populations

Olivier Mousis,^{1*} Magali Deleuil,¹ Artyom Agüichine,¹ Emmanuel Marcq,²
Joseph Naar,^{1,3} Lorena Acuña Aguirre,¹ Bastien Brugger,⁴
and Thomas Gonçalves¹

¹Aix Marseille Univ, CNRS, CNES, LAM, Marseille, France,

²LATMOS/CNRS/Sorbonne Université/UVSQ,

11 boulevard d'Alembert, Guyancourt, F-78280, France

³Laboratoire de Météorologie Dynamique/IPSL, CNRS, Sorbonne Université,

Ecole normale supérieure, PSL Research University, Ecole Polytechnique,

Paris 75005, France,

⁴Department of Astronomy, Cornell University, Ithaca, NY 14853, USA

*To whom correspondence should be addressed; E-mail: olivier.mousis@lam.fr.

With radii ranging between those of the Earth ($1 R_{\oplus}$) and Neptune ($\sim 3.9 R_{\oplus}$), small planets constitute more than half of the inventory of the 4000-plus exoplanets discovered so far¹. This population follows a bimodal distribution peaking at $\sim 1.3 R_{\oplus}$ (super-Earths) and $2.4 R_{\oplus}$ (sub-Neptunes), with few planets in between^{2,3}. Smaller planets are sufficiently dense to be rocky, but those with radii larger than $\sim 1.6 R_{\oplus}$ are thought to display large amounts of volatiles, including in many cases hydrogen/helium gaseous envelopes up to $\sim 30\%$ of the planetary mass^{4,5}. With orbital periods less than 100 days, these low-mass planets are highly irradiated and their origin, evolution, and possible links are still debated⁶⁻¹⁰. Here we show that close-in ocean planets¹¹ affected

by greenhouse effect display hydrospheres in supercritical state, which generate inflated atmospheres without invoking the presence of large H/He gaseous envelopes. We derive a new set of mass-radius relationships for ocean planets with different compositions and different equilibrium temperatures, well adapted to low-density sub-Neptune planets. Our model suggests that super-Earths and sub-Neptunes^{2,3} could belong to the same family of planets. The differences between their interiors could simply result from the variation of the water content in those planets. Close-in sub-Neptunes would have grown from water-rich building blocks compared to super-Earths, and not concurrently from gas coming from the protoplanetary disk. This implies that small planets should present similar formation conditions, which resemble those known for the terrestrial and dwarf planets in the solar system.

Theoretical mass/radius relationships are at odds to explain the composition of the largest members of the small planet population. When available, mass and radius measurements show that super-Earths are sufficiently dense to be rocky while sub-Neptunes fall near curves of planets composed of pure water, suggesting instead a solid core surrounded by a hydrogen/helium gaseous envelope up to $\sim 30\%$ of the planetary mass²⁻¹⁰. However, even though the vast majority of the known small planets are close-in, current mass/radius relationships exclude the physical properties of highly irradiated ocean planets¹¹, whose formation mechanisms do not deviate from those of super-Earths, contrary to sub-Neptunes. This category of planets should be ubiquitous in the universe given the large number of water-rich worlds (Europa, Titan, Enceladus, Pluto, etc) existing in our own solar system.

Here we present new mass/radius relationships of irradiated ocean planets that can easily

explain the large observed radii of the sub-Neptunes population. These relationships are derived from the combination of two one-dimensional models, i.e. a fully differentiated planet interior model¹² and a steam atmosphere model^{13,14} connected at a 1000-bar pressure. The interior model takes as inputs the planetary mass and chemical composition (Mg/Si, Fe/Si mole ratios and water mass fraction), and computes the resulting radius and internal structure of the planet¹². The internal structure relies on the pressure $P(r)$, the temperature $T(r)$, the gravity acceleration $g(r)$, and the density $\rho(r)$ as a function of radius. These quantities are integrated following an iterative scheme until convergence is reached. Along the radius r of the planet, the pressure $P(r)$ is calculated via different equations of state (EOS), which are chosen depending on the material composing the considered layer. The different layers include the core, the lower and upper mantles, the high pressure ice, and a liquid hydrosphere¹². To account for the effects of irradiation, as expected for the close-in population, a water phase in supercritical state has been added to the hydrosphere. For given density and temperature, the supercritical layer pressure is calculated via an EOS (see Methods) obtained from data generated by molecular level computer simulations that consider simple point-charge potential models to which average polarization corrections have been added¹⁵. The resulting EOS (hereafter DZ06) agrees within a $\pm 0.6\%$ deviation with the well-known IAPWS95 formulation¹⁶, which provides an accurate EOS based on experimental data within the $\sim 0\text{--}1.0$ GPa pressure range. At higher pressure, the DZ06 EOS has been shown to compute the pressure within a $\pm 1.3\%$ deviation up to 10.0 GPa, and should remain within a $\pm 5.0\%$ deviation up to 35 GPa, from comparisons with simulated data^{15,17}.

The adiabatic temperature profile within the supercritical layer depends on the Grüneisen parameter, which shows strong dependence with both density and temperature. In the supercritical layer, this parameter is derived from a bilinear interpolation of a grid of data available in the python library for IAPWS standard calculation of water and steam properties¹⁸. This grid

gives a range of Grüneisen parameters for temperatures up to 10^4 K and supercritical water densities up to 2500 kg/m^3 , corresponding to pressures up to ~ 150 GPa, a value exceeding the one at the center of a $20 M_{\oplus}$ planet fully made of water. It shows good agreement with available experimental data up to $1 \text{ GPa}/1273 \text{ K}$ ¹⁶. When deriving this grid, the IAPWS team focused on the extrapolation behavior of the formulation, and ensured it behaves physically at high pressure/temperature domains, which are relevant to (exo)planetary interiors. The Grüneisen parameter's profile is expected to have a correct physical behavior, albeit with increasing uncertainties when going deeper in the planet. However, we find this to be of secondary importance regarding planetary radius as the Grüneisen parameter is basically a proxy of thermal expansivity along pressure variations, which rapidly becomes of second order when pressure increases.

The atmosphere model^{13,14} takes over at water column pressures lower than ~ 1000 bar, where the H_2O envelope behaves more and more like a hot and dense steam atmosphere as the pressure drops. The used model is based on a $T(P)$ profile prescription¹⁹ starting from the 1000-bar level (unsaturated since $T(1000 \text{ bar}) > T_{\text{critical}}$) upwards, assuming a dry adiabat, and switching optionally to a moist adiabat (where $T(P) = T_{\text{saturation}}(P)$) if/when saturation reaches unity. Once the temperature reaches the skin temperature T_{skin} , which is related to the equilibrium temperature T_{eq} via $T_{\text{skin}} = T_{\text{eq}}/2^{1/4}$, an isothermal radiative mesosphere $T = T_{\text{skin}}$ is assumed up to the 0.1 Pa topmost level. Moreover, steam is not treated as an ideal gas, and the EOS is taken instead from the NBS/NRC steam tables²⁰. This enables a smooth transition of the $T(P)$ profile with the interior model. Altitudes are computed assuming hydrostatic equilibrium. Shortwave and thermal fluxes are then computed using 4-stream approximation. Gaseous (line and continuum) absorptions are computed using the k -correlated method. Rayleigh opacity is also included. $T(1000 \text{ bar})$ is iteratively chosen so that the thermal flux at the top of the atmosphere is equal to σT_{eq}^4 . We finally chose the radius/altitude of the 20 mbar level as the observable, transiting radius²¹.

Figure 1 displays the pressure and temperature profiles (hereafter (P, T) profiles) of hydrospheres of 1–15 M_{\oplus} supercritical ocean planets with equilibrium temperatures of 300, 650, and 1200 K, superimposed onto the water phase diagram. The (P, T) profiles expand from the base of the hydrosphere to the top of the H_2O -dominated atmosphere set to 0.1 Pa. Most of the hydrospheres remain in the supercritical regime and those of smallest planets are located well below ice VII, with a fluid-ice VII transition law valid up to 60 GPa²² in the water phase diagram. Beyond this pressure range, the phase change from supercritical to high pressure ices (VII or X) is neglected because the temperature/pressure region remains widely unknown in this region.

Figure 2 represents the mass/radius relationships of supercritical ocean planets calculated in the 0.6–20 M_{\oplus} range for equilibrium temperatures of 300, 650, and 1200 K, corresponding to distances of 0.72, 0.15, and 0.04 AU from a solar-type star, respectively, assuming an Earth-like albedo. The presence of a thick H_2O -dominated atmosphere generates a strong runaway greenhouse effect causing the presence of a supercritical hydrosphere, even if the equilibrium temperature of the planet is lower than the critical temperature of water ($T_{\text{critical}} \sim 650$ K). Because the core-mantle boundary is not firmly defined at very high pressure and temperature²³, we assume here the core and mantle form a unique magma phase of mantelic composition^{13,14}. Figure 2 shows that sub-Neptunes can be well matched by mass/radius curves corresponding to ocean planets with significant supercritical hydrospheres.

Our model suggests that super-Earths and sub-Neptunes^{2,3} could belong to the same family of planets, rather than being distributed in two distinct families, i.e. rocky and Neptune-like planets. Sub-Neptunes would be richer in water and, because of the proximity to their host star, the strong insolation associated to runaway greenhouse effect in their atmospheres generates inflated supercritical hydrospheres, compared to similar bodies with a very low water content located at higher distances to the star. We also note that planets possessing exactly the masses

and radii of Uranus and Neptune could be matched by ocean planets if these latter contain more than 70% of supercritical water, depending on their orbital distance and the type of their host star. Our model does not require the accretion of sub-Neptunes from gas coming from the protoplanetary disk. It implies that both super-Earths and sub-Neptunes would have formed from the accretion of building blocks in a manner similar to those known for the terrestrial and dwarf planets in the solar system. Sub-Neptunes would have grown from water-rich building blocks beyond the snowline in protoplanetary disks and would have then migrated inwards. On the opposite, super-Earths would have grown in water-depleted regions of protoplanetary disks.

This first quantitative exploration of the role of supercritical water in planetary envelopes, which underlines the importance of composition in case of strong irradiation, will be extended by the development of a model describing the planets' interior and atmosphere in a more consistent way. This work also highlights the need for improved EOS in the high pressure and high temperature regime of the water phase diagram.

Methods

Equation of state of supercritical water

The EOS of supercritical water used in this study is written as¹⁵:

$$Z = \frac{PV}{RT} = 1 + \frac{BV_c}{V} + \frac{CV_c^2}{V^2} + \frac{DV_c^4}{V^4} + \frac{EV_c^5}{V^5} + \frac{FV_c^2}{V^2} \times \left(\beta + \frac{\gamma V_c^2}{V^2} \right) \exp \left(-\frac{\gamma V_c^2}{V^2} \right), \quad (1)$$

where $R = 83.14467 \text{ cm}^3 \text{ bar}/(\text{K mol})$ is the universal gas constant. Parameters B , C , D , E , and F in Eq. 1 are calculated via the following equations:

$$B = a_1 + \frac{a_2}{T_r} + \frac{a_3}{T_r^2} \quad (2)$$

$$C = a_4 + \frac{a_5}{T_r^2} + \frac{a_6}{T_r^3} \quad (3)$$

$$D = a_7 + \frac{a_8}{T_r^2} + \frac{a_9}{T_r^3} \quad (4)$$

$$E = a_{10} + \frac{a_{11}}{T_r^2} + \frac{a_{12}}{T_r^3} \quad (5)$$

$$F = \frac{\alpha}{T_r^3} \quad (6)$$

$$T_r = \frac{T}{T_c} \quad (7)$$

$$F = \frac{RT_c}{P_c} \quad (8)$$

Table 1: EoS Parameters

Parameter	
a_1	$4.68071541 \times 10^{-02}$
a_2	$-2.81275941 \times 10^{-01}$
a_3	$-2.43926365 \times 10^{-01}$
a_4	$1.10016958 \times 10^{-02}$
a_5	$-3.86603525 \times 10^{-02}$
a_6	$9.30095461 \times 10^{-02}$
a_7	$-1.15747171 \times 10^{-05}$
a_8	$4.19873848 \times 10^{-04}$
a_9	$-5.82739501 \times 10^{-04}$
a_{10}	$1.00936000 \times 10^{-06}$
a_{11}	$-1.01713593 \times 10^{-05}$
a_{12}	$1.63934213 \times 10^{-05}$
α	$-4.49505919 \times 10^{-02}$
β	$-3.15028174 \times 10^{-01}$
γ	$1.25000000 \times 10^{-02}$

where T_c and P_c are the critical temperature and critical pressure respectively. Here, $T_c = 647.25$ K, and $P_c = 221.19 \text{ cm}^3/\text{mol}$. Parameters a_1 - a_{12} , α , β , and γ are summarized in Table 1. We refer the reader to the study of Duan & Zhang (2006) for details.

References and Notes

1. NASA Exoplanet Archive, <https://exoplanetarchive.ipac.caltech.edu/index.html> (2019)
2. Fulton, B. J., and 12 colleagues. The California-Kepler Survey. III. A Gap in the Radius Distribution of Small Planets. *The Astronomical Journal* 154, 109 (2017).
3. Fulton, B. J., Petigura, E. A. The California-Kepler Survey. VII. Precise Planet Radii Leveraging Gaia DR2 Reveal the Stellar Mass Dependence of the Planet Radius Gap. *The Astronomical Journal* 156, 264 (2018).
4. Lopez, E. D., Fortney, J. J., Miller, N. How Thermal Evolution and Mass-loss Sculpt Populations of Super-Earths and Sub-Neptunes: Application to the Kepler-11 System and Beyond. *The Astrophysical Journal* 761, 59 (2012).
5. Rogers, L. A. Most 1.6 Earth-radius Planets are Not Rocky. *The Astrophysical Journal* 801, 41 (2015).
6. Venturini, J., Helled, R. The Formation of Mini-Neptunes. *The Astrophysical Journal* 848, 95 (2017).
7. Weiss, L. M., Marcy, G. W. The Mass-Radius Relation for 65 Exoplanets Smaller than 4 Earth Radii. *The Astrophysical Journal* 783, L6 (2014).
8. Dorn, C., and 7 colleagues. A generalized Bayesian inference method for constraining the interiors of super Earths and sub-Neptunes. *Astronomy and Astrophysics* 597, A37 (2017).
9. Jin, S., Mordasini, C. Compositional Imprints in Density-Distance-Time: A Rocky Composition for Close-in Low-mass Exoplanets from the Location of the Valley of Evaporation. *The Astrophysical Journal* 853, 163 (2018).

10. Zeng, L., and 15 colleagues. Growth model interpretation of planet size distribution. *Proceedings of the National Academy of Science* 116, 9723 (2019).
11. Léger, A., and 11 colleagues. A new family of planets? “Ocean-Planets”. *Icarus* 169, 499 (2004).
12. Brugger, B., Mousis, O., Deleuil, M., Deschamps, F. Constraints on Super-Earth Interiors from Stellar Abundances. *The Astrophysical Journal* 850, 93 (2017).
13. Marcq, E., Salvador, A., Massol, H., Davaille, A. Thermal radiation of magma ocean planets using a 1-D radiative-convective model of H₂O-CO₂ atmospheres. *Journal of Geophysical Research (Planets)* 122, 1539 (2017).
14. Marcq, E. A simple 1-D radiative-convective atmospheric model designed for integration into coupled models of magma ocean planets. *Journal of Geophysical Research (Planets)* 117, E01001 (2012).
15. Duan, Z., Zhang, Z. Equation of state of the H₂O, CO₂, and H₂O–CO₂ systems up to 10 GPa and 2573.15 K: Molecular dynamics simulations with ab initio potential surface. *Geochemica et Cosmochimica Acta* 70, 2311–2324 (2006).
16. Wagner, W., Pruß, A. The IAPWS Formulation 1995 for the Thermodynamic Properties of Ordinary Water Substance for General and Scientific Use. *Journal of Physical and Chemical Reference Data* 31, 387 (2002).
17. Duan, Z., Møller, N., Weare, J. H. A general equation of state for supercritical fluid mixtures and molecular dynamics simulation of mixture PVTX properties. *Geochimica et Cosmochimica Acta* 60, 1209 (1996).
18. <https://pypi.org/project/iapws/#description>

19. Kasting, J. F. Runaway and moist greenhouse atmospheres and the evolution of Earth and Venus. *Icarus* 74, 472 (1988).
20. Haar, L., Gallagher, J., Kell, G., and National Standard Reference Data System (U.S.). NBS/NRC Steam Tables: Thermodynamic and Transport Properties and Computer Programs for Vapor and Liquid States of Water in SI Units, Hemisphere Publ. Corp., Washington, D. C. (1984).
21. Grimm, S. L., and 25 colleagues. The nature of the TRAPPIST-1 exoplanets. *Astronomy and Astrophysics* 613, A68 (2018).
22. Frank, M.R., Fei, Y., Hu, J. Constraining the equation of state of fluid H₂O to 80 GPa using the melting curve, bulk modulus, and thermal expansivity of Ice VII. *Geochimica et Cosmochimica Acta* 68, 2781–2790 (2004).
23. Hakim, K., and 6 colleagues. A new ab initio equation of state of hcp-Fe and its implication on the interior structure and mass-radius relations of rocky super-Earths. *Icarus* 313, 61 (2018).
24. <http://www.iapws.org/relguide/MeltSub.html>

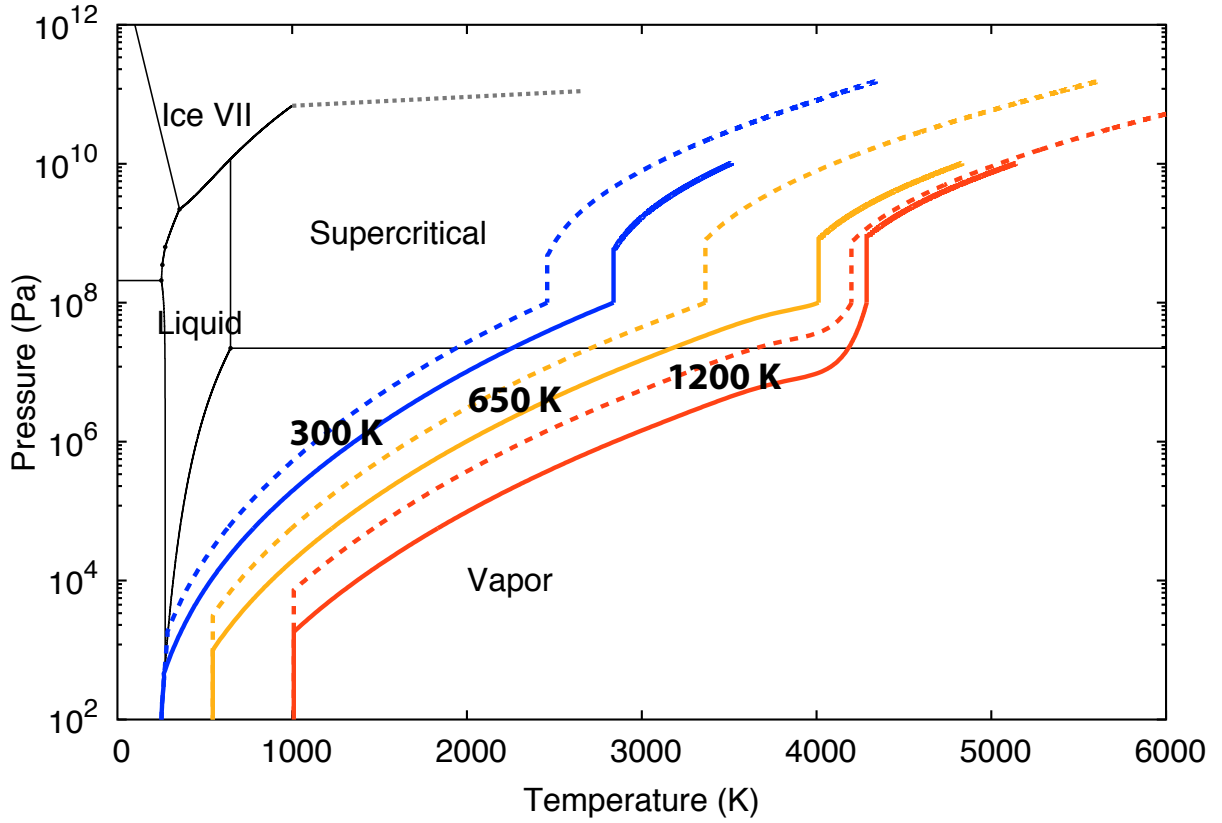


Figure 1: Pressure and temperature profiles of hydrospheres of 1 and 15 M_{\oplus} supercritical ocean planets with equilibrium temperatures of 300, 650, and 1200 K superimposed onto the water phase diagram. Colored solid and dashed curves correspond to 1 and 15 M_{\oplus} planets, respectively. The fluid–ice VII transition law is fitted from data between 3 and 60 GPa²². The grey dashed line delimits an hypothetical transition between the supercritical phase and high pressure ice (see text). The other phase-change laws are collected from a compilation of thermodynamic data¹⁶, and from the website of the International Association for the Properties of Water and Steam (IAPWS)²⁴.

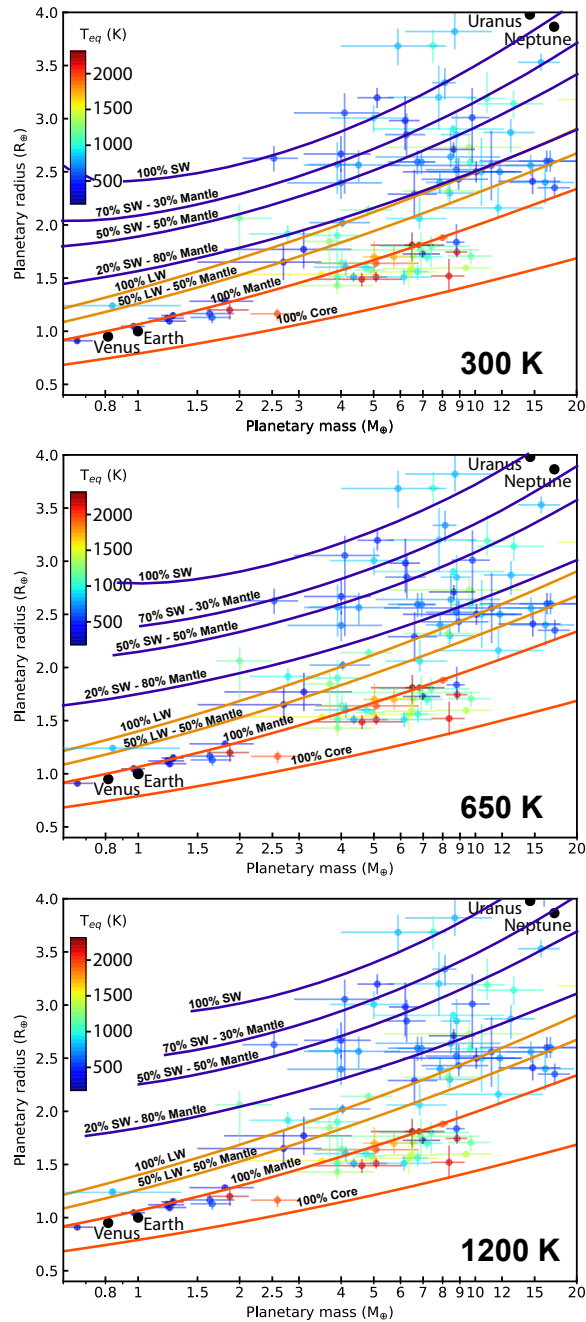


Figure 2: Mass-radius diagrams determined for exoplanets with masses in the $0.6\text{--}20 M_{\oplus}$ range, and equilibrium temperatures of 300 K, 650 K, and 1200 K. Mass-radius curves are calculated for several planetary compositions: 100% core and 100% mantle (red curves), liquid water (LW) hydrosphere (brown curves) and supercritical water (SW) hydrosphere (blue curves) topping mantle-like composition interiors. Planetary data are taken from the NASA exoplanet archive and updated to 20th July 2019. Hydrostatically unstable atmospheres (defined when the altitude at 0.1 Pa tends towards infinity) around the hotter and smaller planets are excluded from the mass-radius relationships.